

Low-energy neutrinos at off-axis from a standard beta-beam

R. Lazauskas,^{1,*} A. B. Balantekin,^{2,†} J. H. de Jesus,^{2,‡} and C. Volpe^{1,§}

¹*Institut de Physique Nucléaire, F-91406 Orsay cedex, France*

²*Department of Physics, University of Wisconsin, Madison, WI 53706, USA*

(Dated: May 26, 2019)

We discuss a scenario to extract up to 150 MeV neutrinos at a standard beta-beam facility. We show that the high-energy component of the neutrino fluxes can be subtracted through a specific combination of the response of two off-axis detectors. A systematic analysis of the neutrino fluxes using different detector geometries is presented, as well as a comparison with the expected fluxes at a low-energy beta-beam facility. The presented option could offer an alternative way to perform low-energy neutrino experiments.

PACS numbers: 13.15.+g, 14.60.Lm, 23.40.Bw, 29.90.+r

Keywords: Low-energy neutrino interactions, beta-beams, off-axis neutrino fluxes

I. INTRODUCTION

Low-energy neutrino sources play an important role in neutrino physics. Depending on the applications, one typically can choose between single-spectrum but intense, sources such as reactors, or multi-spectra sources with lower intensity such as the proposed low-energy beta-beam facilities. In such facilities one can study neutrino-nucleus interactions, fundamental neutrino properties, and perform various electroweak tests.

Low-energy neutrino-nucleus interactions are important in several contexts. The response of the chemical detectors to low-energy neutrino sources such as the Sun and supernovae is dependent on their neutrino capture cross sections. Neutrino-nucleus cross sections are an important ingredient in understanding various astrophysical phenomena, for example, the dynamics of the core-collapse supernovae [1], calculating the yields of the supernova r-process nucleosynthesis [2], and assessing the formation possibility of a black hole from the fossil abundances of the r-process elements [3]. These interactions are also an important input into models of gamma-ray bursts [4, 5] and their understanding is fundamental to the observation of neutrino signals from astrophysical sources [6, 7]. In particle physics, low-energy neutrinos can be used as probes to test the electroweak component of the Standard Model [8].

Low-energy beta-beam facilities first proposed in Ref. [9] yield pure beams of electron neutrinos or antineutrinos produced through the decay of radioactive ions circulating in a storage ring [10, 11]. Several applications utilizing low-energy beta-beams have been discussed in the literature concerning neutrino-nucleus scattering [12, 13, 14], electroweak tests of the Standard Model [15, 16, 17, 18, 19], as well as core-collapse supernova physics [9, 20].

An extensive analysis of the physics potential of a beta-beam facility is currently undergoing, in parallel with the feasibility design study. One of the primary goals of a standard beta-beam facility is to test CP-violation in the lepton sector. Currently, experiments are in the planning stage to measure the third mixing angle, θ_{13} , at reactors [21, 22]. Beta-beam facilities will be able to measure this angle as well as the associated CP-violating Dirac phase. Various scenarios for beta-beam facilities have been considered as far as the measurement of θ_{13} and CP violation in the lepton sector is concerned [24, 25, 26, 27, 28, 29, 30, 31, 32, 33, 34, 35, 36, 37, 38]. Lepton number violating interactions are discussed in Ref. [39] (for a review, see Ref. [11]).

In this paper we discuss an alternative to using low-energy beta-beams, namely the possibility of extracting low-energy neutrino fluxes emitted from a standard beta-beam facility, using a specific off-axis configuration. The basic idea is that if a detector is placed away from the principal axis of the storage ring, it will detect the least energetic neutrinos emitted from the parent nucleus. We also explore possible geometries for such off-axis detectors.

The main body of this paper is Section II. In this section we derive the formulas and discuss the neutrino flux profiles for three different scenarios: the original low-energy beta-beam scenario, used as reference (Section II A); one off-axis detector in a standard beta-beam facility (Section II B); and two off-axis detectors in a standard beta-beam facility (Section II C). A discussion of our results is then given in Section III.

*Electronic address: lazauska@lpsc.in2p3.fr

†Electronic address: baha@physics.wisc.edu

‡Electronic address: jhjesus@physics.wisc.edu

§Electronic address: volpe@ipno.in2p3.fr

II. NEUTRINO FLUX PROFILES

Zucchelli first proposed the idea to use boosted radioactive ions as a new method to produce pure, collimated and well known electron (anti)neutrino fluxes [10]. The ions are stored in a storage ring where they decay. To get the fluxes one needs to integrate over the storage ring straight sections and the volume of the detector. The average neutrino flux at the detector is therefore given by (the precise formalism can be found in [12])

$$\tilde{\Phi}_{tot}(E_\nu) = f\tau \int_0^Z \frac{dl}{L} \int_V \frac{\Phi_{lab}(E_\nu, \hat{r})}{4\pi r^2} dV, \quad (1)$$

where L is the total and Z is the straight section lengths of the storage ring. In the stationary regime, the mean number of ions in the storage ring is $\gamma\tau f$, where $\tau = t_{1/2}/\ln 2$ is the lifetime of the parent nucleus and f is the number of injected ions per unit time. In Eq. (1), the integration is performed over the detector volume V and the nearest storage ring straight section, with \vec{r} being the vector connecting two points in the storage ring and the detector.

Using Eq. (1), the total number of events per unit time with energies up to E_{\max} , in the detector, is

$$dN/dt = n \int_0^{E_{\max}} \tilde{\Phi}_{tot}(E_\nu) \sigma(E_\nu) dE_\nu, \quad (2)$$

with n being the number of target particles per unit volume and $\sigma(E_\nu)$ the cross section. Neutrino-nucleus cross sections at low energies are approximately proportional to the square of the impinging neutrino energy. This motivates the introduction of the quantity

$$\bar{N} = \int_0^{E_{\max}} \tilde{\Phi}_{tot}(E_\nu) E_\nu^2 dE_\nu, \quad (3)$$

to estimate the number of expected events independent of the detector material and the duration of data acquisition.

The calculations we present are performed assuming parameters from the currently ongoing feasibility study [23, 41]. For the original beta-beam scenario, we assume a storage ring of total length $L = 6580$ m with straight sections of length $Z = 2501$ m. The ${}^6\text{He}$ expected intensity to produce antineutrino fluxes is $f = 2.53 \times 10^{13}$ ions/s. For the low-energy beta-beam, we consider $L = 1885$ m and $Z = 678$ m with $f = 2.65 \times 10^{12}$ ions/s [42].

A. Reference scenario: the low-energy beta-beam facility

The idea of a low-energy beta-beam facility producing neutrinos in the 100 MeV energy range has been first proposed in [9]. The disposal of a devoted storage ring would probably be the ideal tool for low-energy neutrino physics [12]. The potential of such a facility has been stressed in several papers [9, 13, 14, 16, 17, 18, 19, 20]. In Table I, we summarize the characteristics of the corresponding fluxes for the case of antineutrinos¹ resulting from the decay of $\gamma = 7$ and $\gamma = 14$ ${}^6\text{He}$ ions. The maximal energy of the neutrinos in these cases are 55 MeV and 100 MeV, respectively. We consider a cylindrical detector with $r = 4.5$ m (radius) and $h = 15$ m (depth), placed 10 m from the end of the straight section, as done in Refs. [16, 17].

γ	$\langle E \rangle$	$\sqrt{\langle E^2 \rangle - \langle E \rangle^2}$	$E(\tilde{\Phi}_{\max})$	$\tilde{\Phi}_{\max}/10^9$	$\bar{N}/10^{13}$
7	22.8	17.1	20.7	24.5	40.8
14	42.6	19.9	37.0	28.4	351

TABLE I: Average energy, energy dispersion, peak-energy, peak-flux and \bar{N} value of Eq. (3) at a cylindrical detector placed 10 m away from a low-energy beta-beam running ${}^6\text{He}$ ions at $\gamma = 7$ and $\gamma = 14$. Energies are in units of MeV, the flux in units of $\text{m MeV}^{-1}\text{s}^{-1}$, while \bar{N} is in units of $\text{m MeV}^2\text{s}^{-1}$.

¹ The calculations presented in this paper are for antineutrinos only. However, they are also valid for neutrinos emitted at beta-beam facilities. In what follows, we refer to neutrinos as a generic term.

B. Off-axis neutrino fluxes at a standard beta-beam facility

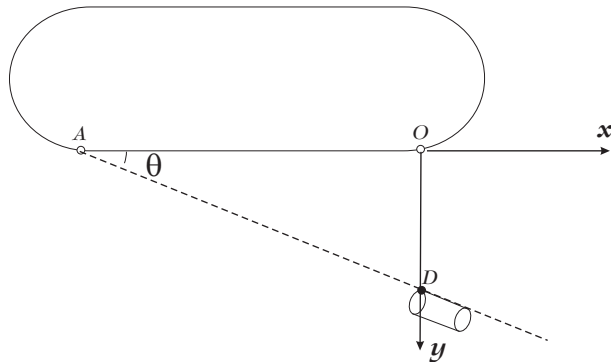


FIG. 1: The location of the single off-axis detector D is shown relative to the standard beta-beam storage ring with straight section AO .

Let us now consider the possibility of extracting low-energy neutrinos from the standard beta-beam facility [10], where ions are boosted at $\gamma = 60 - 100$ and the neutrinos produced with energies up to² 600 MeV. The accelerated ions emit the highest energy neutrinos along the boost direction. Therefore, by placing the detector off the storage ring straight section axis (Figure 1), one gets rid of the highest energy component of the neutrino flux. The highest energy neutrinos reaching the point D in Fig. 1 will be emitted from the most distant point in the storage ring straight section (point A). If one wishes that only neutrinos with energy less or equal to E_{cut} arrive at point D , the angle $\theta = \angle ADO$ has to satisfy the condition

$$\theta = \arccos \left[\frac{\gamma - (Q - m_e)/E_{\text{cut}}}{\sqrt{\gamma^2 - 1}} \right], \quad (4)$$

where Q is the Q -value of the reaction. The actual location of the detector depends on the desired antineutrino *cut-off* energy.

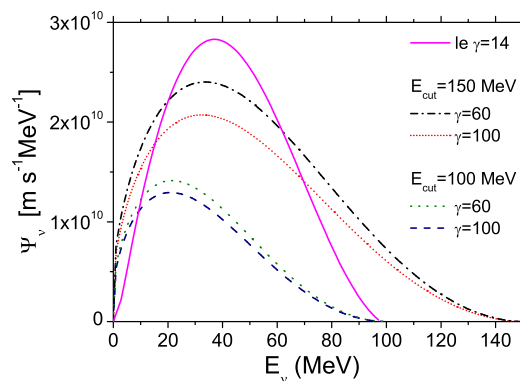


FIG. 2: Off-axis antineutrino fluxes ($\times 20$) evaluated at point D of Fig. 1 for two different ion boosts and neutrino energy cuts. The neutrino flux from a low-energy beta-beam (le) at $\gamma = 14$ is shown for comparison.

In Figure 2, we compare the off-axis antineutrino fluxes evaluated at point D , which lies on the perpendicular to the storage ring straight section derived from the turning point O ($x = 0$; see Fig. 1). The distance $y = AD = AO \cdot \tan \theta$

² Note that the corresponding storage ring can not be used to store ions with low γ , considered in Sec. II A

is determined using Eq.(4) and by constraining the maximum energy of the neutrinos (E_{cut}) reaching that point. The presented results correspond to the cases where the ${}^6\text{He}$ ions are boosted at $\gamma = 60$ and $\gamma = 100$, and when E_{cut} is set to 100 and 150 MeV. In particular, if $\gamma = 60$ and $E_{\text{cut}} = 100$ MeV, the distance y is 74.7 meters (Fig. 1). If the ions are stored at $\gamma = 100$, y reduces to 61.4 meters, since the neutrino beam is more collimated. The main characteristics of such fluxes are summarized in Tables II and III. In order to compare these results with the low-energy beta-beam fluxes of Table I, the value of $\tilde{\Phi}_{\text{max}}$ and \bar{N} are normalized by the same detector volume.

E_{cut}	$\langle E \rangle$	$\sqrt{\langle E^2 \rangle - \langle E \rangle^2}$	$E(\tilde{\Phi}_{\text{max}})$	$\tilde{\Phi}_{\text{max}}/10^9$	$\bar{N}/10^{13}$	y
100	32.7	19.6	21.0	0.64	4.88	61.4
150	49.6	29.5	32.5	1.03	27.1	48.0

TABLE II: Same as Table I but for an off-axis flux at a point in space with coordinates $x = 0$ and y such that the maximum energy of the neutrinos is E_{cut} (value in the first column). The ions are boosted at $\gamma = 100$. Energies are in units of MeV, the flux in units of $\text{m MeV}^{-1}\text{s}^{-1}$, \bar{N} is in units of $\text{m MeV}^2\text{s}^{-1}$ and y in meters.

E_{cut}	$\langle E \rangle$	$\sqrt{\langle E^2 \rangle - \langle E \rangle^2}$	$E(\tilde{\Phi}_{\text{max}})$	$\tilde{\Phi}_{\text{max}}/10^9$	$\bar{N}/10^{13}$	y
100	32.9	19.7	21.4	0.70	5.41	74.7
150	50.2	29.6	33.5	1.20	32.2	56.0

TABLE III: Same as Table III but for $\gamma = 60$.

From Tables II and III, one can see that the off-axis antineutrino flux profiles are determined by the choice of E_{cut} (which determines the angle θ) and come out to be not very sensitive to the boost of the ions. Note, however, that \bar{N} – which is related to the number of events – is reduced by 10% to 20% when γ changes from 100 to 60. The flux shapes are strongly asymmetric, centered at low energies, and having a long high-energy tail.

E_{cut}	$\langle E \rangle$	$\sqrt{\langle E^2 \rangle - \langle E \rangle^2}$	$E(\tilde{\Phi}_{\text{max}})$	$\tilde{\Phi}_{\text{max}}/10^9$	$\bar{N}/10^{13}$	y
100	29.3	17.7	18.5	0.57	3.08	61.4
150	43.6	26.3	28.0	0.87	15.6	48.0

TABLE IV: Same as Table II but for a cylindrical detector with $r = 4.5$ m and $h = 15$ m.

Let us briefly discuss how the off-axis antineutrino flux changes close to the point D of Fig. 1. First, the flux is clearly symmetric with respect to a rotation around the straight section AO ; it does not vary significantly along the line AD for distances of order $y \ll AO$. Nevertheless, the flux is very sensitive to variations of the angle θ and reduces significantly once one moves away from the storage ring straight section. Therefore, in order to have the highest count rate at the detector, one should place it by aligning its longitudinal part with AD . In Tables IV and V we present the results for a cylindrical detector with³ $r = 4.5$ m and $h = 15$ m. One can see that taking into account the physical size of the detector reduces the flux at the peak only by about 10%; however, it strongly affects its high-energy tail and therefore the events count rate, associated with the quantity \bar{N} .

From these results, it is clear that both the off-axis flux at the peak intensity and the related number of events \bar{N} , are considerable smaller – by factors of 20-100 – than those of the low-energy beta-beam option. Such drastic reduction clearly makes this option hardly realizable for low-energy neutrino physics applications.

C. Alternative scenario: two off-axis detectors at a standard beta-beam facility

In order to remove the high-energy neutrinos from the flux, the off-axis detector should be placed relatively far away from the straight section ($y > 50$ m). This renders the intensities very low. It is worth noting that the neutrino

³ This is the same detector geometry as considered in the low-energy beta-beam scenario of Section II A.

E_{cut}	$\langle E \rangle$	$\sqrt{\langle E^2 \rangle - \langle E \rangle^2}$	$E(\tilde{\Phi}_{\text{max}})$	$\tilde{\Phi}_{\text{max}}/10^9$	$\tilde{N}/10^{13}$	y
100	30.3	18.2	19.5	0.63	3.79	74.7
150	45.6	27.1	30.2	1.05	21.2	56.0

TABLE V: Same as Table III but for a cylindrical detector with $r = 4.5$ m and $h = 15$ m.

flux has almost the same energy dependence at any point along the AD (Figure 1). Furthermore, the flux intensities along this line are inversely proportional to the distance from point A . However, if one gets closer to point A , the signal start being contaminated by the high-energy neutrinos emitted from the bending part of the storage ring.

To overcome this difficulty, we introduce a novel technique which consist in comparing the response of two off-axis detectors, placed in a specific configuration close to the storage ring axis. By using the subtraction procedure described below, one is able to extract the low-energy antineutrino flux and gain one order of magnitude in the intensity.

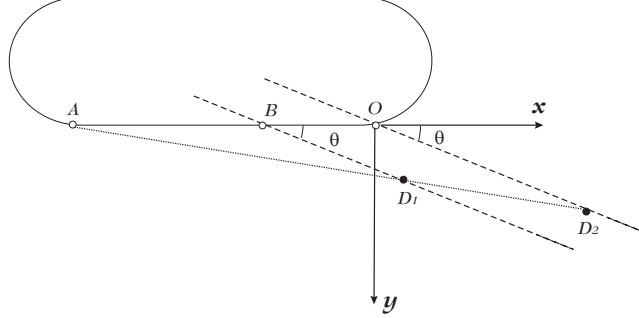


FIG. 3: Schematic view of the two off-axis detector locations, D_1 and D_2 , relative to the straight section of the beta-beam storage ring, AO .

Let us consider the neutrino fluxes in two points D_1 and D_2 , as shown in Figure 3. We split the neutrino flux $\Psi_{D_1}(E_\nu)$ in point D_1 in two parts: one component produced in the segment AB of the storage ring, i.e. $\Psi_{D_1}^{(AB)}(E_\nu)$, and the other produced in the segment BO , $\Psi_{D_1}^{(BO)}(E_\nu)$. Since the triangles ABD_1 and AOD_2 are similar, the flux fraction $\Psi_{D_1}^{(AB)}(E_\nu)$ in point D_1 is proportional to the neutrino flux $\Psi_{D_2}(E_\nu)$ in point D_2 :

$$\Psi_{D_1}^{(AB)}(E_\nu) = \Psi_{D_2}(E_\nu) \frac{AO}{AB} \quad (5)$$

The flux $\Psi_{D_1}^{(BO)}(E_\nu)$ can be obtained combining the responses of the two detectors located in D_1 and D_2 , by using the following subtraction procedure:

$$\Psi_{D_1}^{(BO)}(E_\nu) = \Psi_{D_1}(E_\nu) - \Psi_{D_2}(E_\nu) \frac{AO}{AB} \quad (6)$$

Note that this flux contains only neutrinos with energies less than E_{cut} , set by Eq. (4). The subtracted flux of Eq. (6) has a similar energy dependence as the flux at the point

$$x = AD_1 \cos \theta - AO, \quad (7)$$

$$y = AD_1 \sin \theta, \quad (8)$$

but its intensity is higher by a factor of y/y_{D_1} .

In Section II B we found that a y -distance of 48 m to 75 m is required in order to get low-energy neutrinos from the off-axis flux (Figure 2 and Tables II and III). Here, the detector D_1 can be placed very close to the storage ring. This implies a neutrino flux intensity enhancement by ~ 10 . The position of the detector at D_2 with respect to the position of the detector at D_1 is fixed by the choice of the desired maximal neutrino energy (E_{cut}) of the subtracted flux. The same arguments are valid for the realistic, large size detectors: one should place two detectors having the same shape, but the detector in D_2 should have its linear dimensions larger by a factor of OD_2/BD_1 than the detector in D_1 .

Once one considers a finite size detector, it is clear that the remote regions of the detector will see much less neutrinos than the regions close to the subtraction axis (BD_1 for the detector located at D_1 , or AD_2 for the detector

located at D_2). For large size detectors their shape and its orientation should play an important role. Probably the best detector geometry would be the long and thin, hollow inside, conus. For such a geometry, one will have the subtracted fluxes very similar to the ones shown in Figure 2, but with an intensity higher by $\sim y/y_{D_1}$. The cone-like detector geometry has been considered in a recent theoretical study [40]. Nevertheless, the technical realization of such detectors is expected to be difficult.

We now consider the neutrino fluxes at four large detectors, having standard shapes (spherical or cylindrical), whose dimensions are given in Table VI. All four detectors are taken to have the same volume; detector type d_2 also has the same shape as the reference detector of Section II A. In Figure 4, we compare the subtracted neutrino fluxes for the four detectors. The cylindrical detectors are considered to be placed longitudinally along the subtraction axis (BD_1 for the detector located at D_1 or AD_2 for the detector located at D_2) as shown in Figure 3. In the case of spherical detectors, the center of the first one is placed at $x = R_{\text{det}}$ and $y = R_{\text{det}} + 5$ m. For the disc detector, the upper surface touches the subtraction axis and is inclined along it. One can see that the longest detector (d_1) picks the most neutrino flux: two times more than the spherical detector (d_4).

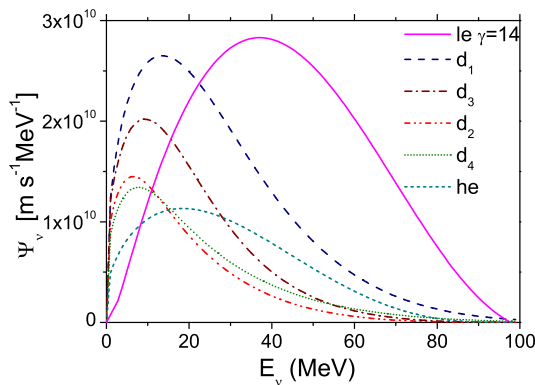


FIG. 4: Comparison of the different low-energy neutrino fluxes obtained with a standard beta-beam, exploiting two detectors off-axis (Figure 3) and the subtraction method described in the text (these fluxes are multiplied by 6). The different curves correspond to four different detector geometries, namely the cylinder-sausage (d_1), the cylinder-normal (d_2), the cylinder-disc (d_3), and the spherical (Table VI). As a comparison, the flux from a low-energy beta-beam (le), and for a single off-axis detector d_2 (he) are given. The last flux is multiplied by 20.

The flux profile is even more asymmetric than for the single off-axis detector case (Figure 2). Note that the average energy is pushed towards much lower energies (around 10-20 MeV) compared to the low-energy beta-beam flux. The expected intensities are significantly higher than in the case of the single off-axis detector, but still a few times weaker than for the low-energy beta-beam discussed in Section II A.

Name	Type	Parameters	Volume (m ³)
d ₁	Cylinder-Sausage	r = 2.25 m h = 60.0 m	954
d ₂	Cylinder-Normal	r = 4.50 m h = 15.0 m	954
d ₃	Cylinder-Disc	r = 9.00 m h = 3.75 m	954
d ₄	Spherical	r = 6.11 m	954

TABLE VI: Four different 954-ton detector geometries

In Figure 5, we compare the subtracted neutrino fluxes for type- d_1 detectors, when one is placed at $y = 5$ m from the storage ring straight section and its twin detector is placed in such a way that the subtracted neutrino flux is either $E_{\text{cut}} = 100$ MeV or 150 MeV. The ions in the storage ring are considered to be boosted to $\gamma = 100$ and 60. One can see that for large size detectors, a lower ion boost is advantageous. For example, one gains more than 30%

in intensity by reducing the boost from 100 to 60.

In Figure 6, we show how the subtracted flux intensities vary by placing the detector at different distances from the storage ring (the closest point are $y=5, 7.5$ and 10 m away from the storage ring, respectively). If the detector has a small size compared to y , the subtracted intensity should scale as $1/y$. On the other hand, for the large detector we consider one gains much less in intensity by placing it closer to the straight section (e.g. $y=10$ and $y=5$ m fluxes differ only by 50%).

	$\gamma = 100$					$\gamma = 60$				
	$\langle E \rangle$	$\sqrt{\langle E^2 \rangle - \langle E \rangle^2}$	$E(\tilde{\Phi}_{\max})$	$\tilde{\Phi}_{\max}/10^9$	$N/10^{13}$	$\langle E \rangle$	$\sqrt{\langle E^2 \rangle - \langle E \rangle^2}$	$E(\tilde{\Phi}_{\max})$	$\tilde{\Phi}_{\max}/10^9$	$N/10^{13}$
d ₁	21.3	18.5	13.50	4.42	19.2	28.7	19.1	15.0	6.09	31.4
d ₂	18.5	14.3	6.50	2.42	3.42	25.3	14.6	7.29	3.31	5.36
d ₃	20.4	14.7	9.32	3.36	6.43	21.4	15.1	10.3	4.60	10.1
d ₄	15.0	12.3	4.50	1.78	1.32	24.0	20.6	5.43	2.42	2.12

TABLE VII: Same as Table I for the four different detector types of Table VI. The fluxes were obtained with the subtraction method described in the text for a standard beta-beam facility running ${}^6\text{He}$ ions at $\gamma = 100$ and $\gamma = 60$, and for a *cut-off* energy of 100 MeV.

	$\gamma = 100$					$\gamma = 60$				
	$\langle E \rangle$	$\sqrt{\langle E^2 \rangle - \langle E \rangle^2}$	$E(\tilde{\Phi}_{\max})$	$\tilde{\Phi}_{\max}/10^9$	$N/10^{13}$	$\langle E \rangle$	$\sqrt{\langle E^2 \rangle - \langle E \rangle^2}$	$E(\tilde{\Phi}_{\max})$	$\tilde{\Phi}_{\max}/10^9$	$N/10^{13}$
d ₁	39.0	26.3	20.6	5.44	70.9	41.27	26.8	23.3	7.63	116.
d ₂	28.2	21.4	10.8	3.05	15.3	29.95	22.0	12.7	4.31	25.8
d ₃	31.1	21.9	15.0	4.22	28.2	33.07	22.5	17.2	5.93	47.4
d ₄	23.0	18.5	7.79	2.23	6.13	24.8	19.2	9.30	3.16	10.9

TABLE VIII: Same as Table VII but for a *cut-off* energy of 150 MeV.

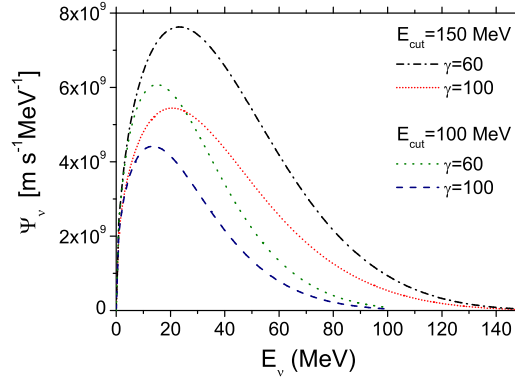


FIG. 5: Neutrino fluxes obtained by placing two detectors d₁ (Table VI) off-axis and using the subtraction method described in the text. The different curves correspond to two ion boosts and maximum neutrino energy cutoff. The first detector is located at $y=5$ m.

As we were completing this paper, the authors of Ref. [40] presented an analysis of how neutrino spectral shapes change at low-energy beta-beams depending on the detector geometry and different locations within the same detector. The analyses presented in the current paper and in Ref. [40] are complementary in exploring the potentials of standard and low-energy beta-beam facilities, respectively.

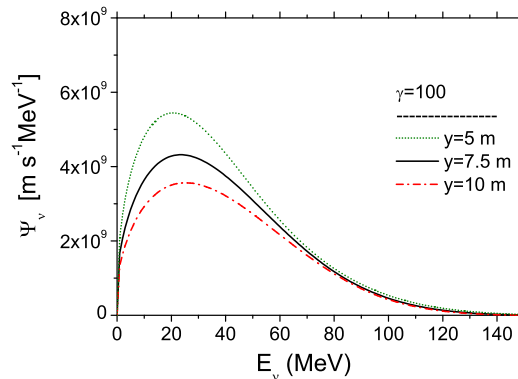


FIG. 6: Same as Figure 5 but for different y locations.

III. CONCLUSIONS

In this article we explored the feasibility of extracting low-energy neutrinos from the standard beta-beam facility by placing detectors at off-axis. We found that with a single off-axis detector the low-energy neutrino fluxes extracted are rather small. With two off-axis detectors, after suitable subtractions, one can obtain sizable low-energy neutrino fluxes to perform various experiments. In the latter case the energy spectra of the neutrinos are pushed to lower energies than for the low-energy beta-beam. The covered energy range is of interest for fundamental tests and for core-collapse supernovae physics. We also studied the dependence of the flux intensity and energy spectrum on the location and geometry of the detectors.

We conclude that the option of two off-axis detectors at a standard beta-beam facility is a valid alternative to the reference scenario of a low-energy beta-beam facility for the realization of low-energy neutrino experiments.

Acknowledgments

The authors acknowledge the CNRS-Etats Units 2005 and 2006 grants which have been used during the completion of this work. This work was also supported in part by the EURISOL design study, in part by the U.S. National Science Foundation Grant No. PHY-0555231 at the University of Wisconsin, and in part by the University of Wisconsin Research Committee with funds granted by the Wisconsin Alumni Research Foundation. R.L. acknowledges the financial support of the EC under the FP6 "Research Infrastructure Action-Structuring the European Research Area" EURISOL DS Project; Contract No. 515768 RIDS.

-
- [1] A. B. Balantekin and G. M. Fuller, J. Phys. G **29**, 2513 (2003) [arXiv:astro-ph/0309519].
 - [2] B. S. Meyer, G. C. McLaughlin and G. M. Fuller, Phys. Rev. C **58**, 3696 (1998) [arXiv:astro-ph/9809242].
 - [3] T. Sasaqui, T. Kajino and A. B. Balantekin, Astrophys. J. **634**, 534 (2005) [arXiv:astro-ph/0506100].
 - [4] M. Ruffert, H. T. Janka, K. Takahashi and G. Schafer, Astron. Astrophys. **319**, 122 (1997) [arXiv:astro-ph/9606181].
 - [5] J. P. Kneller, G. C. McLaughlin and R. Surman, J. Phys. G: Nucl. Part. Phys. **32**, 443 (2006) arXiv:astro-ph/0410397.
 - [6] P. Vogel and J. F. Beacom, Phys. Rev. D **60**, 053003 (1999) [arXiv:hep-ph/9903554].
 - [7] J. F. Beacom, W. M. Farr and P. Vogel, Phys. Rev. D **66**, 033001 (2002) [arXiv:hep-ph/0205220].
 - [8] G. 't Hooft, Phys. Lett. B **37** (1971) 195.
 - [9] C. Volpe, J. Phys. G **30** (2004) L1 [arXiv:hep-ph/0303222].
 - [10] P. Zucchelli, Phys. Lett. B **532** (2002) 166.
 - [11] C. Volpe, J. Phys. G **34**, R1 (2007) [arXiv:hep-ph/0605033].
 - [12] J. Serreau and C. Volpe, Phys. Rev. C **70** (2004) 055502 [arXiv:hep-ph/0403293].
 - [13] G. C. McLaughlin, Phys. Rev. C **70** (2004) 045804 [arXiv:nucl-th/0404002].
 - [14] C. Volpe, J. Phys. G **31** (2005) 903 [arXiv:hep-ph/0501233].
 - [15] G. C. McLaughlin and C. Volpe, Phys. Lett. B **591** (2004) 229 [arXiv:hep-ph/0312156].

- [16] A. B. Balantekin, J. H. de Jesus and C. Volpe, Phys. Lett. B **634** (2006) 180 [arXiv:hep-ph/0512310].
- [17] A. B. Balantekin, J. H. de Jesus, R. Lazauskas and C. Volpe, Phys. Rev. D **73**, 073011 (2006) [arXiv:hep-ph/0603078].
- [18] A. Bueno, M. C. Carmona, J. Lozano and S. Navas, Phys. Rev. D **74**, 033010 (2006).
- [19] J. Barranco, O. G. Miranda and T. I. Rashba, arXiv:hep-ph/0702175.
- [20] N. Jachowicz and G. C. McLaughlin, Prog. Part. Nucl. Phys. **57**, 350 (2006) [arXiv:nucl-th/0511069]; Phys. Rev. Lett. **96**, 172301 (2006) [arXiv:nucl-th/0604046].
- [21] F. Ardellier *et al.* [Double Chooz Collaboration], arXiv:hep-ex/0606025.
- [22] [Daya Bay Collaboration], arXiv:hep-ex/0701029.
- [23] B. Autin *et al.*, J. Phys. G **29**, 1785 (2003) [arXiv:physics/0306106].
- [24] M. Mezzetto, J. Phys. G **29**, 1771 (2003) [arXiv:hep-ex/0302007].
- [25] M. Mezzetto, Nucl. Phys. Proc. Suppl. **149**, 179 (2005).
- [26] M. Mezzetto, Nucl. Phys. Proc. Suppl. **155**, 214 (2006) [arXiv:hep-ex/0511005].
- [27] J. Burguet-Castell, D. Casper, J. J. Gomez-Cadenas, P. Hernandez and F. Sanchez, Nucl. Phys. B **695**, 217 (2004) [arXiv:hep-ph/0312068].
- [28] J. Burguet-Castell, D. Casper, E. Couce, J. J. Gomez-Cadenas and P. Hernandez, Nucl. Phys. B **725**, 306 (2005) [arXiv:hep-ph/0503021].
- [29] J. E. Campagne, M. Maltoni, M. Mezzetto and T. Schwetz, arXiv:hep-ph/0603172.
- [30] S. K. Agarwalla, A. Raychaudhuri and A. Samanta, Phys. Lett. B **629**, 33 (2005) [arXiv:hep-ph/0505015].
- [31] S. K. Agarwalla, S. Choubey, S. Goswami and A. Raychaudhuri, arXiv:hep-ph/0611233.
- [32] S. K. Agarwalla, S. Choubey and A. Raychaudhuri, arXiv:hep-ph/0610333.
- [33] A. Donini, E. Fernandez, P. Migliozi, S. Rigolin, L. Scotto Lavina, T. Tabarelli de Fatis and F. Terranova, arXiv:hep-ph/0511134.
- [34] A. Donini, E. Fernandez-Martinez, P. Migliozi, S. Rigolin and L. Scotto Lavina, Nucl. Phys. B **710**, 402 (2005) [arXiv:hep-ph/0406132].
- [35] A. Donini, E. Fernandez-Martinez and S. Rigolin, Phys. Lett. B **621**, 276 (2005) [arXiv:hep-ph/0411402].
- [36] A. Donini, D. Meloni and S. Rigolin, JHEP **0406**, 011 (2004) [arXiv:hep-ph/0312072].
- [37] A. Donini, D. Meloni and P. Migliozi, Nucl. Phys. B **646**, 321 (2002) [arXiv:hep-ph/0206034].
- [38] P. Huber, M. Lindner, M. Rolinec and W. Winter, Phys. Rev. D **73**, 053002 (2006) [arXiv:hep-ph/0506237].
- [39] S. K. Agarwalla, S. Rakshit and A. Raychaudhuri, arXiv:hep-ph/0609252.
- [40] P. S. Amanik and G. C. McLaughlin, arXiv:hep-ph/0702207.
- [41] <http://beta-beam-parameters.web.cern.ch/beta-beam-parameters/index.jsp>.
- [42] A. Chancé and J. Payet, private communication.